

# Impact of Zinc Concentration on Fuel Crud in a Simulated Primary Water of PWRs

Hee-Sang Shim<sup>1\*</sup>, Kyeong-Su Kim<sup>1</sup>, Hye Min Park<sup>1</sup>, Jin-Soo Choi<sup>2</sup>, Kyu Min Song<sup>2</sup>, Do Haeng Hur<sup>1</sup>

<sup>1</sup>Nuclear Materials Research Division, KAERI, 989-111 Daedeok-daero, Yuseong-gu, Daejeon 34057, Korea

<sup>2</sup>Central Research Institute, KHNP, 1312-70, Yuseong-daero, Yuseong-gu, Daejeon 34101, Korea

\*Corresponding author: [hshim@kaeri.re.kr](mailto:hshim@kaeri.re.kr)

## 1. Introduction

Corrosion products are released in the various forms such as oxides and ions from the surfaces of structural materials into the primary coolant of pressurized water reactors (PWRs) in operation.

Several corrosion products of nickel, cobalt, and iron are activated by neutron flux in the reactor core and thus increase the radiation dose and occupational radiation exposure in out-of-core region. A part of corrosion products is remained as the deposit on fuel cladding tubes, which is called crud [1, 2] and often results the accumulation of boron in its porous structure [3,4] or increase of local surface temperature. The increased boron content within the crud can cause a shift in the core neutron flux along the length of the fuel assemblies, referred to as axial offset anomaly (AOA) or crud induced power shift (CIPS) [5,6]. In addition, the increase of local surface temperature often induce localized corrosion and fuel failure [7,8]. Therefore, it is important to decrease the released corrosion products in order to minimize the radiation build-up, AOA and fuel failure.

Zinc addition to pressurized water reactor coolant has been applied to minimize the radiation field in reactor coolant system and to mitigate stress corrosion cracking of primary structural materials from 1994 [9]. The beneficial effect of zinc addition in the reduction of radiation field is basically attributed to a decrease of corrosion rates and corrosion product release rates from primary system materials in PWRs [10-12], especially steam generator tubing. Stress corrosion cracking of stainless steels and Ni-based alloys was also mitigated by zinc addition into the primary coolant [13,14]. Recently, it was reported that the low cycle fatigue life of 316 stainless steel significantly increased by zinc addition in a PWR condition [15].

It has also been confirmed that zinc addition does not have an adverse effect on the oxide growth rates and already deposited crud of zirconium-based fuel cladding materials [16,17]. Based on some fuel crud examinations from zinc-injecting plants, it seemed that crud was relatively thin and uniformly distributed along the length of the fuel assemblies compared to that before zinc injection [18]. As described above, numerous studies on zinc addition have been conducted in various concentration from various perspectives. However, publications about the impacts of zinc addition on fuel crud are still scarce in the open literature, possibly because of its high level radiation in operating plants and experimental difficulty in laboratories.

In this study, the effect of zinc addition to simulated

PWR primary coolant on fuel crud, which has similar properties in chemical composition and physical properties with plant crud, was investigated under controlled zinc concentration in water chemistry. The physical and chemical properties of fuel crud was discussed through various analysis.

## 2. Experimental

### 2.1. Preparation of specimen and test solution

The effect of zinc concentration on crud deposited on fuel cladding surface was analyzed in following two-step experiments: 1) thick crud deposition, 2) immersion test in PWR primary water containing different zinc content.

A commercial zirconium alloy tube was used as a fuel cladding material. Its chemical composition and mechanical properties are summarized in Table 1. This tube has a dimension of 9.5 mm in outer diameter (OD), 8.3 mm in inner diameter (ID), and 550 mm in length, respectively. The cladding tube was sequentially degreased in acetone, ethanol, and deionized water after welding one end with zirconium plug. A cartridge heater was inserted into the tube and the gap between tube and cartridge heater was filled with MgO paste.

The simulated PWR primary water is prepared by dissolving LiOH of 2 ppm and H<sub>3</sub>BO<sub>3</sub> of 1,000 ppm into the deionized water. The dissolved oxygen was controlled to be less than 5 ppb and dissolved hydrogen was maintained 35 cc/kg-H<sub>2</sub>O. Crud source for fuel crud deposition was prepared using nickel ethylenediamine tetraacetic acid (EDTA) of 1,500 ppm and iron acetate of 2,000 ppm.

Table 1. Chemical composition and mechanical properties of fuel cladding tube.

Composition (wt%)					Mechanical properties		
Sn	Fe	O	Nb	Zr	YS (MPa)	UTS (MPa)	Elong. (%)
1.0	0.1	0.12	1.0	Bal.	612.5	819.2	15.8

### 2.2. Thick crud deposition test

Thick crud deposition were performed using the KAERI crud deposition loop system as shown in Fig. 1 [19]. The primary coolant recirculated via a high pressure pump, preheater, test section, and heat exchanger with a flow rate of 280 mL/min. The temperature and pressure of primary coolant in the test section were maintained at 325°C and 13 MPa. The heat flux from clad surface was controlled to 65 W/cm<sup>2</sup> to make sub-cooled nucleate

condition [20]. The crud source was injected to the bottom of test section by using a metering pump with a flow rate of 1.0 mL/min. The deposition test was conducted for 10 days crud layer to be thicker than 30  $\mu\text{m}$ .

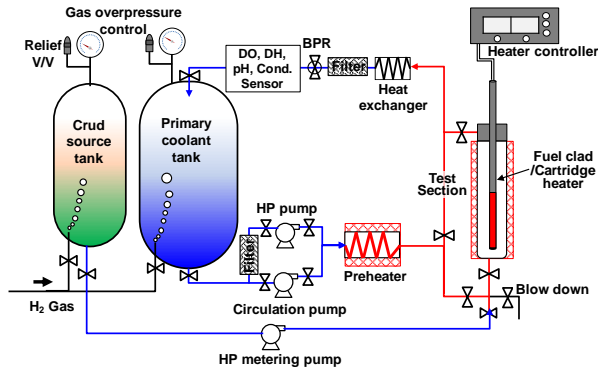


Fig. 1 Schematic of the test loop for thick crud deposition.

### 2.3. Immersion test of fuel cruds

The immersion test of fuel crud was performed using the simulated primary loop system as shown in Fig. 2. The crud-deposited cladding tube prepared by using the crud deposition loop was transferred and mounted to test section of the immersion test loop. A depleted zinc acetate (DZA) was used as a zinc source and dissolved directly into the solution tank. The zinc concentration was 10 ppb and 60 ppb in simulated primary coolant in this work. Two solution tanks of 200 L and 50 L were switched in order to maintain consistently the zinc concentration during experiment.

Other chemistry conditions of primary coolant were the same with the crud deposition experiment. The heat flux from clad surface was maintained to 65  $\text{W}/\text{cm}^2$  and the immersion test was conducted for 500 h.

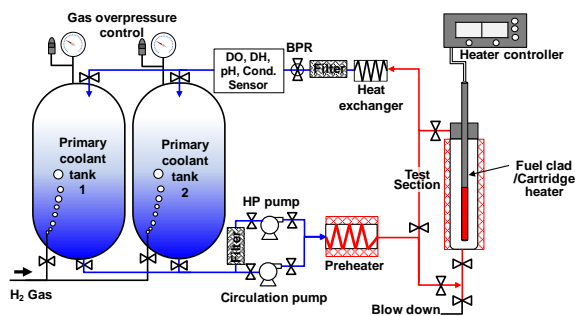


Fig. 2 Schematic of the immersion test loop for fuel crud under Zn injection.

### 2.3. Crud analysis

After the immersion tests in primary coolant containing the zinc content of 10 ppb and 60 ppb, the cladding tube specimens were cut into tubular segments using a tube cutter to analyze the crud.

The morphology of as-deposited crud and its immersed crud was observed using a scanning electron microscope (SEM). The thickness and porosity of crud

layer were evaluated from the cross-sectional images the cross sections, which was machined by a focused ion beam (FIB) technique, by using Lince and ImageJ softwares. Crud particles were detached with a 3M tape from the cladding surfaces for XRD examinations. X-ray diffraction patterns were recorded in the  $2\theta$  range from  $25^\circ$  to  $75^\circ$  with a scanning rate of  $1^\circ/\text{min}$  using a Rigaku SMARTLab high resolution diffractometer with Cu-K $\alpha$  radiation at 40 kV and 300 mA. To prepare transmission electron microscopy (TEM) specimens, the outset crud layer exposed to the coolant was machined using a focused ion beam (FIB) milling technique. Scanning TEM (STEM) images were observed using a FEI Talos F200X microscope operating at a voltage of 200 kV. The elemental mapping and compositions of the crud were analyzed using an energy dispersive X-ray spectroscopy (EDS) equipped in the TEM.

## 3. Results and discussion

Fig. 3 shows the SEM micrographs and XRD pattern of crud deposited on clad for immersion test. Many protruding structures and various size pores were shown in Fig. 3(a). The crud layer was mainly composed of few micrometer and sub-micrometer polyhedral particles as shown in Fig. 3(b). In addition, the large pores as marked in yellow-dashed circles should be a boiling chimney, which is made due to escape of boiling bubbles. It was observed that the deposited crud layer was very porous in cross-sectional image as shown in Fig. 3(c). The characteristic peaks of deposited crud were corresponded to those of spinel nickel ferrite ( $\text{Ni}_{0.4}\text{Fe}_{2.6}\text{O}_4$ , JCPDS No. 87-2336).

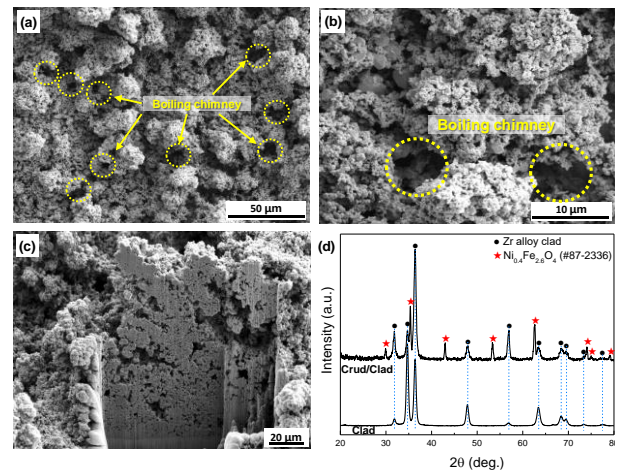


Fig. 3 (a-c) Surface and cross-sectional SEM micrographs of thick crud deposited fuel cladding tube, (d) XRD patterns of clad and crud deposited on clad.

Fig. 4 shows the SEM surface micrographs of the cruds after immersion test in 10 ppb and 60 ppb Zn conditions from as-deposited crud. The surface morphologies of cruds immersed in simulated PWR primary coolant containing Zn content was similar with that of as-deposited crud. This means that the impact of zinc addition on the surface morphologies of crud deposited

on fuel cladding is negligible.

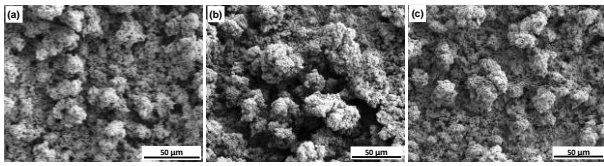


Fig. 4 SEM surface micrographs of the crud: (a) as-deposited crud, (b) crud after immersion test in 10 ppb Zn condition, and (c) crud after immersion test in 60 ppb Zn condition.

The thickness and porosity of crud were evaluated by using Lince and ImageJ software from the SEM cross-sectional images, which was machined by FIB technique. Fig. 5 shows the average thickness and porosity of the crud. The average thickness of as-deposited crud was 65  $\mu\text{m}$  and 34.5%, respectively. The average thicknesses of crud immersed in the primary water containing 10 ppb and 60 ppb Zn were 53  $\mu\text{m}$  and 63  $\mu\text{m}$ , respectively. However, the thickness range of these immersed crud, which is in the range of 35  $\mu\text{m}$  to 73  $\mu\text{m}$ , was in the range of that of as-deposited crud. However, since the thickness of the crud layers consisting of protruding structures and boiling chimneys may vary depending on location, the comparative evaluation of the thickness of these crud would be meaningless.

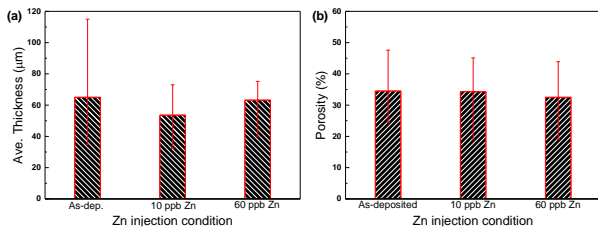


Fig. 5. Average thickness and porosity of crud before and after immersion test in PWR primary coolant containing zinc.

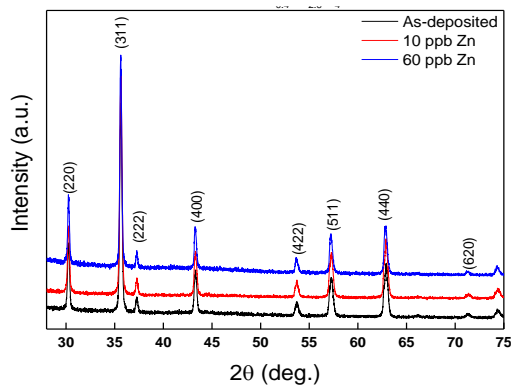


Fig. 6 XRD patterns of crud before and after immersion test in PWR primary coolant containing zinc.

Fig. 6 shows the XRD results of the crud before and after immersion tests. The Miller indices for the peaks were determined by using the relation between  $\sin 2\theta$  values and the combined equation of the Bragg law with the plane-spacing equation for each crystal system. As denoted in the figure, the Bragg planes such as (2 2 0), (3 1 1), (2 2 2), (4 0 0), (4 2 2), (5 1 1), (4 4 0), and (6 2 0) belong to the cubic spinel structure of the Fd-3 m space

group. The most intense peak was observed on the (3 1 1) plane and no other separate peaks were identified by the XRD. All these reflections were consistent with the standard pattern of cubic spinel  $\text{Ni}_{0.4}\text{Fe}_{2.6}\text{O}_4$  (JCPDS Card No. 87-2336).

To better compare the crud compositions, the atomic fractions of Ni and Fe in the crud were calculated based on the STEM-EDS analyses. Fig. 7 shows the STEM image and quantitative elemental mappings for as-deposited crud. The as-deposited crud was an oxide composed of Ni and Fe. Zn was not found in the as-deposited crud. In addition, Ni and Fe were only analyzed in the crud after immersion test in the primary coolant containing Zn as shown in Fig. 8 and 9. This results are well corresponded with the XRD result as shown in Fig. 6. It indicates that the zinc is not migrated into the porous fuel crud or chemically bound with it regardless of zinc concentration in the primary coolant.

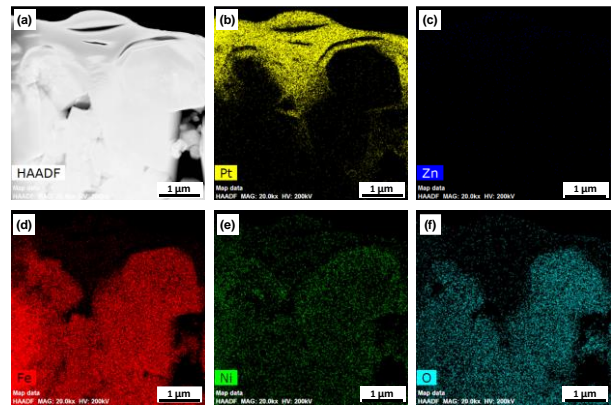


Fig. 7 (a) STEM images and (b-f) TEM-EDS elemental mapping results of as-deposited crud.

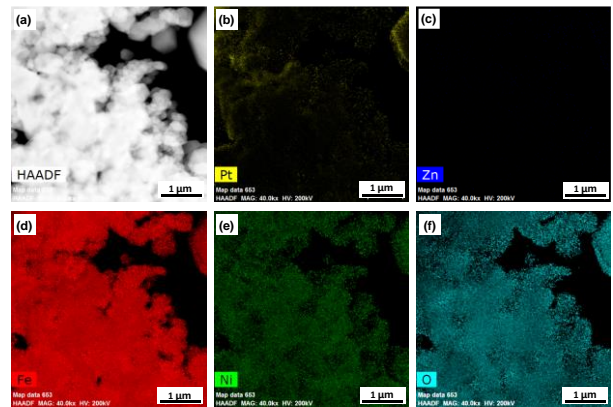


Fig. 8 (a) STEM images and (b-f) TEM-EDS elemental mapping results of crud after immersion test in PWR primary coolant containing 10 ppb Zn.

In our previous paper [19], the zinc is incorporated with the crud structure when it is added in beginning operation stage, and its concentration increases with decreasing Ni content in the spinel nickel ferrite particles as the zinc concentration added into the primary coolant. Furthermore, the quantity of crud deposited on fuel cladding as increases as the zinc concentration increases in the primary coolant. This is caused by that zinc cation

is preferable to substitute better than Ni cation into spinel ferrite structure. In addition, it is because of that the electrostatic repulsive force between the colloidal oxide particles and fuel cladding surface becomes lower as the zinc concentration increases in the primary coolant. However, both physical and chemical properties of already-deposited crud were not changed from that before immersion test in coolant containing zinc. It would possibly be because the immersion time of 500 h is not enough zinc ion to substitute to Ni ion in nickel ferrite crud or the electrostatic force between corrosion product particles and crud surface is weaker than that between those and clad surface.

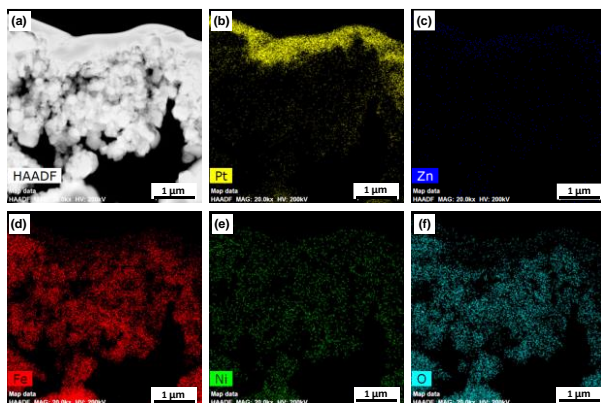


Fig. 9 (a) STEM images and (b-f) TEM-EDS elemental mapping results of crud after immersion test in PWR primary coolant containing 60 ppb Zn.

#### 4. Conclusions

We have investigated the effect of zinc concentration on crud layer deposited on fuel cladding tube through immersion test in simulated primary coolant containing zinc contents of 10 ppb and 60 ppb. The change in surface morphology and porosity of crud layer is not found after immersion test in the primary coolant containing for 500 h. The zinc content was not found in cruds immersed in the primary coolant containing both 10 ppb and 60 ppb zinc. In addition, the XRD characteristic peaks of the immersed cruds in zinc addition are same with that of as-deposited crud. Therefore, it is considered that the zinc added to the primary water does not affect to the crud already deposited on fuel cladding regardless of its concentration at least less than 60 ppb.

#### Acknowledgments

This work was financially supported by the Korea Hydro & Nuclear Power Co., Ltd. of the Republic of Korea (L18S061000). This work was also supported by the National Research Foundation of Korea (NRF) grant funded by the government of the Republic of Korea (2017M2A8A4015159).

#### REFERENCES

- [1] M. P. Short, The particulate nature of the crud source term in light water reactors, *J. Nucl. Mater.* Vol. 509, pp. 478, 2018.
- [2] S. Odar, Crud in PWR/VVER coolant, Vol. 1, Technical Report, ANT Int'l, Sweden, 2014.
- [3] J. A. Sawicki, Evidence of  $\text{Ni}_2\text{FeBO}_5$  and  $\text{m-ZrO}_2$  precipitates in fuel rod deposits in AOA-affected high boiling duty PWR core, *J. Nucl. Mater.*, Vol. 374, pp. 248, 2008.
- [4] I. Betova, M. Bojinov, P. Kinnunen, T. Sarrio, Zn injection in Pressurized Water Reactors-laboratory tests, field experience and modelling, Research Report, VTT-R-05511-11, VTT, Finland, 2011.
- [5] J. Deshon, D. Hussey, B. Kendrick, J. McGurk, J. Secker, M. Short, Pressurized water reactor fuel crud and corrosion modeling, *JOM* Vol. 63 (8), pp. 64, 2011.
- [6] S. Uchida, Y. Asakura, H. Suzuki, Deposition of boron on fuel rod surface under sub-cooled boiling conditions - an approach toward understanding AOA occurrence, *Nucl. Eng. Des.* Vol. 241, pp. 2398, 2011.
- [7] N. Cinosi, I. Haq, M. Bluck, S. P. Walker, The effective thermal conductivity of crud and heat transfer from crud-coated PWR fuel, *Nucl. Eng. Des.* Vol. 241, pp. 792, 2011.
- [8] K. Edsinger, C. R. Stanek, B. D. Wirth, Light water reactor fuel performance: current status, challenges, and future high fidelity modelling, *JOM* Vol. 63, pp. 49, 2011.
- [9] S. Bushart, PWR Operating Experience with Zinc Addition and the Impact on Plant Radiation Fields, EPRI, Palo Alto, USA, 1003389, 2003.
- [10] S. Holdsworth, F. Scenini, M. G. Burke, G. Bertali, T. Ito, Y. Wada, H. Hosokawa, N. Ota, M. Nagase, The effect of high-temperature water chemistry and dissolved zinc on the cobalt incorporation on type 316 stainless steel oxide, *Corr. Sci.* Vol. 140, pp. 241, 2018.
- [11] X. Liu, X. Wu, E.-H. Han, Electrochemical and surface analytical investigation of the effects of Zn concentrations on characteristics of oxide films on 304 stainless steel in borated and lithiated high temperature water, *Electrochim. Acta* Vol. 108, pp. 554, 2013.
- [12] S. E. Ziemniak, M. Hanson, Zinc treatment effects on corrosion behavior of 304 stainless steel in high temperature, hydrogenated water, *Corr. Sci.* Vol. 48, pp. 2525, 2006.
- [13] H. Kawamura, H. Hirano, S. Shirai, H. Takamatsu, T. Matsunaga, K. Yamaoka, K. Oshinden, H. Takiguchi, Inhibitory effect of zinc addition to high temperature hydrogenated water on mill-annealed and prefilmed Alloy 600, *Corrosion* Vol. 56, pp. 623, 2000.
- [14] L. Zhang, K. Chena, J. Wang, X. Guo, D. Dua, P. L. Andresen, Effects of zinc injection on stress corrosion cracking of cold worked austenitic stainless steel in high-temperature water environments, *Scr. Mater.* Vol. 140, pp. 50, 2017.
- [15] H. S. Kim, H. B. Lee, J. Chen, C. Jang, T. S. Kim, G. L. Stevens, K. Ahluwalia, Effect of zinc on the environmentally-assisted fatigue behavior of 316 stainless steels in simulated PWR primary environment, *Corr. Sci.* Vol. 151, pp. 97, 2019.
- [16] R. S. Pathania, B. Cheng, M. Dove, R. E. Gold, C. A. Bergmann, Evaluation of zinc addition to the primary coolant of Farley-2 PWR, Proc. Int'l Symposium Fontevraud IV, SFEN, Fontevraud, pp. 959, 1998.
- [17] E. Kolstad, W. J. Symons, K. Bryhn-Intebrigsten, B. C. Oberlander, Evaluation of Zinc Addition on Fuel Cladding Corrosion at the Halden Test Reactor, EPRI, Palo Alto, USA, TR-106357, 1996.
- [18] J. Gorman, Overview Report on Zinc Addition in Pressurized Water Reactors, EPRI, Palo Alto, USA, 1009568, 2004.

- [19] K. S. Kim, S. H. Baek, H.-S. Shim, J. H. Lee, D. H. Hur, Effect of zinc addition on fuel crud deposition in simulated PWR primary coolant conditions, *Annals, Nucl. Energy* Vol.146, pp. 107643, 2020.
- [20] H. Kawamura, Effect of Low DH Concentration on Crud Deposition on heated Zircaloy-4 in Simulated PWR Primary Water, *Proc. Int'l Conf. Nucl. Plant Chemistry, Paris, France, 2012.*